A new equivalent circuit model for on-chip spiral transformers in CMOS RFICs*

Wei Jiaju(韦家驹), Wang Zhigong(王志功)†, Li Zhiqun(李智群), and Tang Lu(唐路)

Institute of RF- & OE-ICs, Southeast University, Nanjing 210096, China

Abstract: A new compact model has been introduced to model on-chip spiral transformers. Unlike conventional models, which are often a compound of two spiral inductor models (i.e., the combination of two coupled Π or 2-Π sub-circuits), our new model only uses 12 elements to model the whole structure in the form of T topology. The new model is based on the physical meaning, and the process of model derivation is also presented. In addition, a simple parameter extraction procedure is proposed to get the elements' values without any fitting and optimization. In this procedure, a new method has been developed for the parameter extraction of the ladder circuit, which is commonly used to represent the skin effect. In order to verify the model's validity and accuracy, we have compared the simulated and measured self-inductance, quality factor, coupling coefficient and insertion loss, and an excellent agreement has been found over a broad frequency range up to the resonant frequency.

Key words: transformer; T-model; equivalent circuit; ladder; spiral; RFIC

DOI: 10.1088/1674-4926/33/5/055007 **EEACC:** 2570

1. Introduction

On-chip spiral transformers are valuable passive components in radio-frequency integrated circuits (RFICs), such as voltage-controlled oscillators[1], power amplifiers[2], and low-noise amplifiers[3]. To represent the electrical performance of on-chip transformers, a frequency-independent equivalent circuit model is needed in common circuit simulators such as SPICE. Meanwhile, a minimum number of lumped elements should be used to accelerate the modeling and simulation while providing sufficient modeling flexibility. In other words, there is a trade-off between compactness, flexibility and accuracy in the modeling of on-chip transformers.

In recent years, many kinds of equivalent circuit models have been developed for on-chip transformers based on different physical layouts[4−12]. To the best of the authors' knowledge, most of the models developed consist of two coupled Π or 2-Π sub-circuits for each inductor coil in the transformer. Although these models are intuitive and accurate, the model structures are complex and make the parameter extraction very difficult. Thus, some of the models' parameters are totally or partly determined by fitting and optimization procedures. In addition, some literatures provide closed-form expressions for on-chip transformers and make the models scalable. But some expressions are merely empirical formulas which depend on specific layout and fabrication process. Besides, deviations in the fabrication process will also lead to inaccuracy.

This paper proposes a new compact T-model for on-chip interleaved transformers, and it can achieve a high accuracy over a broad frequency range with ease.

2. Phenomenon and consideration

In order to gain more insights into the mechanism of coupling between the primary and secondary coils, we compare the characteristics of the primary coil in two configurations by using electromagnetic simulations. As shown in Fig. 1(a), the primary coil is simulated solely by removing the secondary part and forming a "naked" primary coil. In Fig. 1(b), the configuration consists of both coils while the secondary coil is set as a floating part.

The different responses with regard to different configurations are depicted in Fig. 2, and we note that the presence of the secondary coil will decrease the primary coil's self-resonance frequency. According to the conventional models, this phenomenon will be attributed to the secondary coil's capacitive part, which works via the mutual capacitance between two coils. On the other hand, it can be seen that the secondary coil will also decrease the primary coil's quality factor at high frequencies. This is expected to be due to the magnetic-field-resulted eddy currents in the floating coil.

From the above discussions, we can find that a spiral coil in the transformer is more than a simple coil even though the other coil is set as a floating part. The presence of the secondary coil makes its existence known by adding its parasitics to the primary part. The conventional models are designed to partition the transformer's two coils to the states when the other coil is

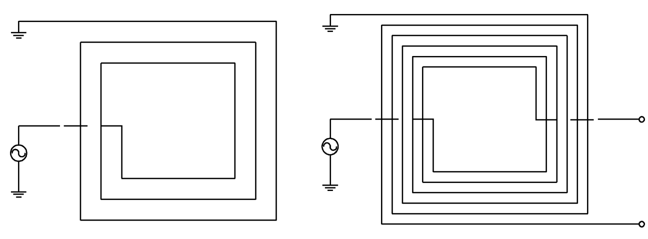
(a) (b)

Fig. 1. Two configurations for the primary coil. (a) "Naked" primary coil. (b) A floating secondary coil.

* Project supported by the National Natural Science Foundation of China (No. 61106024).

† Corresponding author. Email: zgwang@seu.edu.cn

Received 25 December 2011

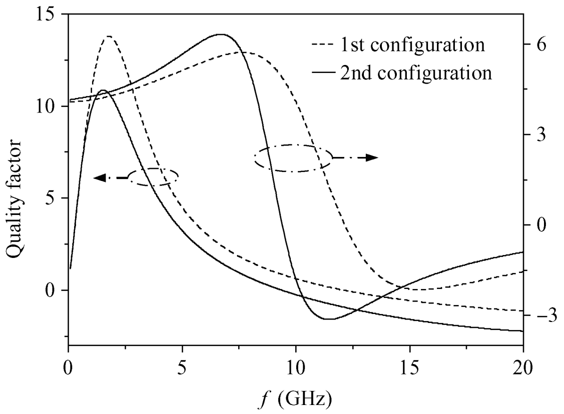

Fig. 2. Characteristics of the primary coil in two configurations.

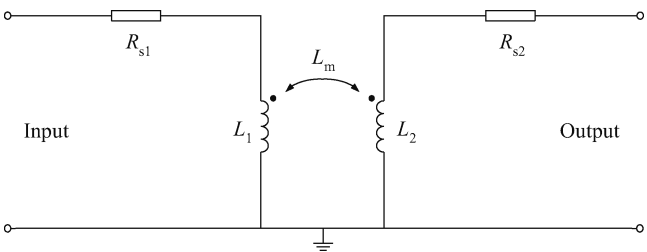

Fig. 3. Physical model in the low frequency band.

removed (i.e. the configuration in Fig. 1(a)). Thus it makes the model complex and difficult to determine its parameters (especially the mutual ones). On the contrary, our new model tries to integrate into one coil with the other coil's parasitics. This integration idea will avoid the detailed partition process and make the new model highly compact.

3. Model derivation

Based on the physical meaning, our new model comes from the conventional model and makes some reasonable equivalent conversions. The new model's construction process is described below.

In the low frequency band, the physical transformer model can be described in Fig. 3. As shown in this figure, R_{si} and L_i $(i = 1, 2)$ denote the DC resistance and inductance of the corresponding coil, respectively. $L_{\rm m}$ is introduced to account for the mutual inductance between the primary and secondary coils.

Using decoupling technology, we can easily get the equivalent circuit model in the following figure. Compared with the Π-topology in Fig. 3, the derived model demonstrates itself as a standard T-topology.

Based on the T-topology shown in Fig. 4, we take some additional parasitic effects for the high frequencies into account, and then, a new compact model is formed to represent on-chip transformers. In our new model (shown in Fig. 5), the magnetizing inductance $L_{\rm m}$ is introduced to account for the lossless and linear magnetic coupling between the two spiral windings. $C_{\rm ox}$ represents the dielectric capacitance for the entire transformer, and the transformer's electric dissipations in the conductive substrate are modeled by the elements $C_{\rm sub}$ and $R_{\rm sub}$.

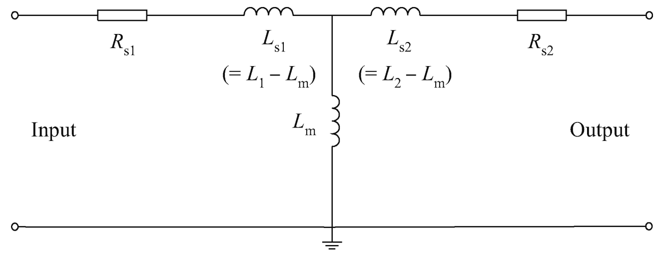

Fig. 4. Decoupling conversion.

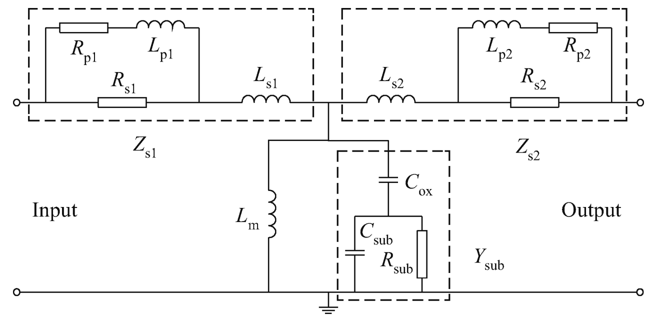

Fig. 5. New compact model for transformers.

Besides, in order to account for the ohmic losses and the leakage of the magnetic flux between the coils, two ladder circuits are added. In the ladders, L_{si} $(i = 1, 2)$ denotes the leakage inductance of the corresponding coil, and the sub-circuit consisting of $R_{\rm p\mathit{i}}$, R_{si} and $L_{\rm p\mathit{i}}$ $(i = 1, 2)$ represents the corresponding coil's ohmic losses in the presence of the other coil over a broad frequency band.

According to our new model, it seems as if the input and output ports of the transformer are physically connected together. Actually, the isolation of DC current flow between the primary and secondary coils can be achieved in our new model. As demonstrated below, the new model and the transformer's physical feature are closely linked.

Firstly, according to the model verification (i.e. Section 5), an excellent agreement between the measured and modeled figures-of-merit (especially the insertion loss) has been found over a broad frequency range. This shows our new model can be applied in the AC condition.

Secondly, in the DC condition, we can easily get the simplified circuit (i.e. Fig. 6(a)) by shorting (opening) the inductive (capacitive) elements in our new model. Then, according to the resistance converting relation "Δ–Y", the seemly connected circuit in Fig. 6(a) can be equivalently converted to the circuit in Fig. 6(b) and a clear isolation shows.

4. Parameter extraction procedure

4.1. Model decomposition

The first step of the parameter extraction is to convert the measured two-port S-parameters into the corresponding Z-parameters. As shown in Fig. 5, the new model demonstrates itself as a standard T topology. Using the definition of Z-parameters, we can get the following relations

$$Z_{\rm s1} = Z_{11} - (Z_{12} + Z_{21})/2, \quad (1)$$

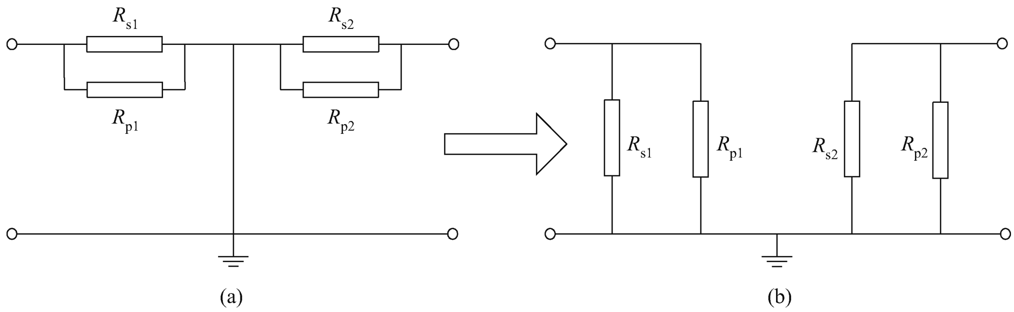

Fig. 6. Model conversion in the DC condition. (a) Before conversion. (b) After conversion.

$$Z_{s2} = Z_{22} - (Z_{12} + Z_{21})/2, \tag{2}$$

$$Y_{sub} = 2/(Z_{12} + Z_{21}) - 1/j\omega L_m. \tag{3}$$

At the DC frequency, we can get L_m as

$$L_m = \left.\frac{\mathrm{Im}\,[(Z_{12} + Z_{21})/2]}{\omega}\right|_{\omega\to 0}. \tag{4}$$

4.2. Extraction for the shunt branch

The shunt branch is composed of 3 elements, i.e., C_{ox}, C_{sub} and R_{sub}. Using the real part and imaginary part of the admittance (i.e., Y_{sub}), Reference [13] introduced two useful characteristic functions for the parameter extraction as

$$f_1(\omega) = \frac{\omega^2}{\mathrm{Re}(Y_{sub})}, \tag{5}$$

$$f_2(\omega) = \frac{\mathrm{Im}(Y_{sub})}{\mathrm{Re}(Y_{sub})}\omega. \tag{6}$$

In this paper, we directly use the method developed in Ref. [13] to extract the values of C_{ox}, C_{sub} and R_{sub}, and the detailed process is omitted.

4.3. Extraction for the ladder circuits

The real and imaginary parts of the ladder's impedance (i.e., Z_{si} $(i = 1, 2)$) can be written as

$$rz_i \triangleq \mathrm{Re}(Z_{si}) = \frac{R_{si}(R_{si}R_{pi} + R_{pi}^2 + L_{pi}^2\omega^2)}{(R_{si} + R_{pi})^2 + L_{pi}^2\omega^2}, \tag{7}$$

$$lz_i \triangleq \frac{\mathrm{Im}(Z_{si})}{\omega} = L_{si} + \frac{L_{pi}R_{si}^2}{(R_{si} + R_{pi})^2 + L_{pi}^2\omega^2}. \tag{8}$$

Combining Eqs. (7) and (8) properly, we developed two new characteristic functions as

$$\begin{aligned} y_1 &\triangleq \frac{\omega^2 - \omega_0^2}{(lz_i/rz_i) - (lz_i/rz_i)_{\omega\to\omega_0}} \\ &= -\frac{(R_{si}R_{pi} + R_{pi}^2 + L_{pi}^2\omega^2)(R_{si}R_{pi} + R_{pi}^2 + L_{pi}^2\omega_0^2)}{L_{pi}^2[L_{pi}R_{si} + L_{si}(R_{si} + R_{pi})]} \\ &= p_{1i} + p_{2i}\omega^2, \end{aligned} \tag{9}$$

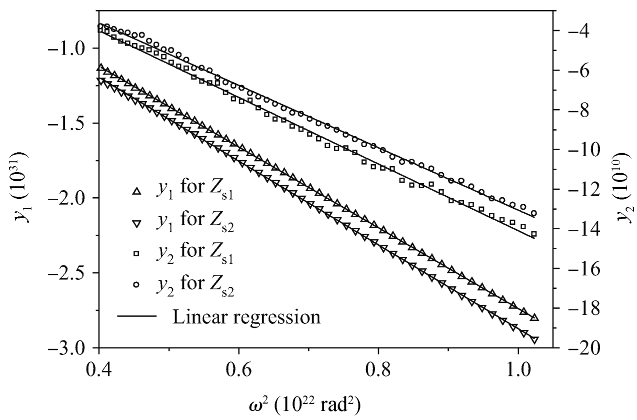

Fig. 7. y_1 and y_2 as a function of ω^2 based on measurements.

$$\begin{aligned} y_2 &\triangleq \frac{(\omega^2 - \omega_0^2)(lz_i - lz_{i\,\omega\to\omega_0})}{rz_i - rz_{i\,\omega\to\omega_0}} \\ &= -\frac{L_{pi}(\omega^2 - \omega_0^2)}{R_{si} + R_{pi}} \\ &= q_{1i} + q_{2i}\omega^2. \end{aligned} \tag{10}$$

Demonstrated in Fig. 7 (ω_0 has been set as the minimum frequency in the measurement), y_1 and y_2 exhibit a good linear dependence on ω^2. Thus, p_{1i}, p_{2i}, q_{1i} and q_{2i} $(i = 1, 2)$ can be extracted by linear regression easily. Then, we can get

$$k_i = p_{2i}/(p_{1i}q_{2i}^2) - 1, \tag{11}$$

$$R_{pi} = rz_{i\,\omega\to 0}(1 + 1/k_i), \tag{12}$$

$$R_{si} = R_{pi}k_i, \tag{13}$$

$$L_{pi} = (R_{si} + R_{pi})(-q_{2i}), \tag{14}$$

$$L_{si} = lz_{i\,\omega\to\omega_0} - L_{pi}R_{si}^2/\left[(R_{si} + R_{pi})^2 + L_{pi}^2\omega_0^2\right]. \tag{15}$$

It should be emphasized here that the ladder circuit is commonly used to represent the skin effect in the modeling of many

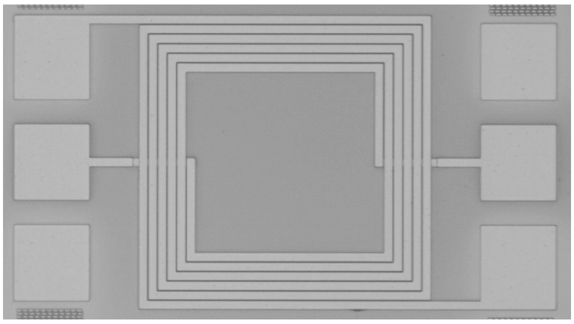

Fig. 8. Top view of a fabricated on-chip transformer.

Table 1. Extracted model parameters.

Parameter	Value
R_{s1}	46.86 Ω
R_{s2}	46.55 Ω
L_{s1}	0.20 nH
L_{s2}	0.20 nH
R_{p1}	2.86 Ω
R_{p2}	2.85 Ω
L_{p1}	0.71 nH
L_{p2}	0.73 nH
L_m	3.2 nH
R_{sub}	88.34 Ω
C_{ox}	129.84 fF
C_{sub}	110.20 fF

passive components, such as on-chip transmission lines, inductors, baluns, etc. Many literatures have made their efforts to extract the ladder's parameters. In Ref. [14], the constant resistance ratio and inductance ratio are estimated for round wires by empirical formulas, and Reference [13] obtains the ladder's parameters based on iterations. In contrast, the method proposed in this paper (i.e., Eqs. (7)–(15)) can extract the parameters of the ladder circuit without any optimization and it will also not be confined to specific structures.

5. Model verification

As shown in Fig. 8, an on-chip interleaved transformer has been fabricated in a 90 nm 1P9M CMOS process with substrate resistivity of about 10 Ω·cm and top metal thickness of 3 μm. The line width and line spacing are 8 μm and 1.5 μm, respectively, and the outer diameter of the transformer is 291 μm. Two-port S-parameters were measured and the pad parasitics were de-embedded using the open pad structure.

The extracted model parameters are listed in Table 1. Although the transformer layout is designed to be absolutely symmetrical, it still exhibits a slight asymmetry, which can be demonstrated by different parameters for two ladder circuits in Table 1.

We use Z-parameters converted from the measured S-parameters to extract the self-inductance (L_p and L_s), quality factors (Q_p and Q_s), coupling coefficient (k) and insertion loss (IL) as functions of frequency. These parameters are calculated using the following expressions:

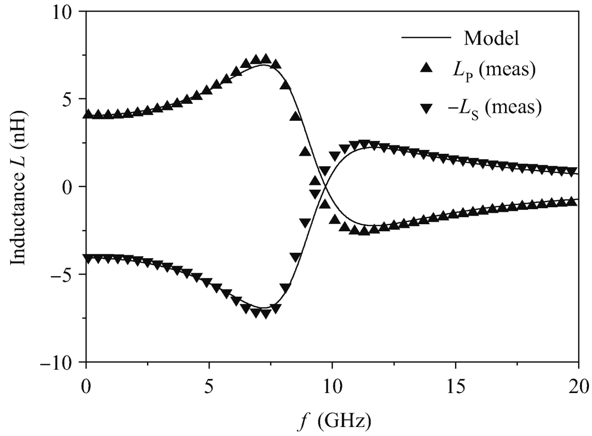

Fig. 9. Inductance comparison.

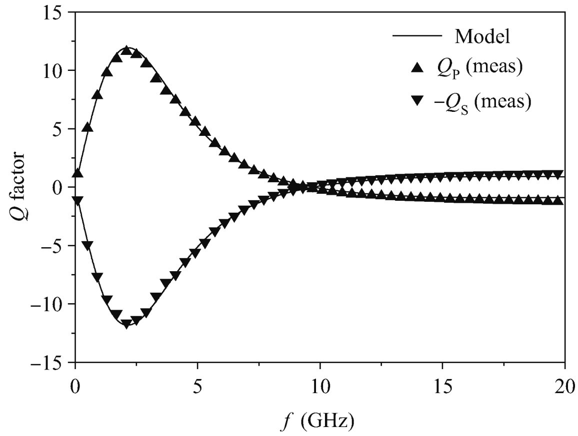

Fig. 10. Quality factor comparison.

$$L_p = \frac{\mathrm{Im}(Z_{11})}{2\pi f}, \tag{16}$$

$$L_s = \frac{\mathrm{Im}(Z_{22})}{2\pi f}, \tag{17}$$

$$Q_p = \frac{\mathrm{Im}(Z_{11})}{\mathrm{Re}(Z_{11})}, \tag{18}$$

$$Q_s = \frac{\mathrm{Im}(Z_{22})}{\mathrm{Re}(Z_{22})}, \tag{19}$$

$$k = \sqrt{\frac{\mathrm{Im}(Z_{12})\mathrm{Im}(Z_{21})}{\mathrm{Im}(Z_{11})\mathrm{Im}(Z_{22})}}, \tag{20}$$

$$\mathrm{IL} = 20\lg(|S_{21}|). \tag{21}$$

In order to verify the model's validity and accuracy, we have compared the modeled and measured L_s, L_p, Q_p, Q_s, k and IL. As demonstrated from Fig. 9 to Fig. 12, an excellent agreement has been found between our new model and the measurement over a broad bandwidth up to the resonant frequency. It should be emphasized here that our new model only contains 12 elements, while the number of elements in conventional transformer models[15] is usually larger than 14. On the other hand, our new model avoids the detailed partition process

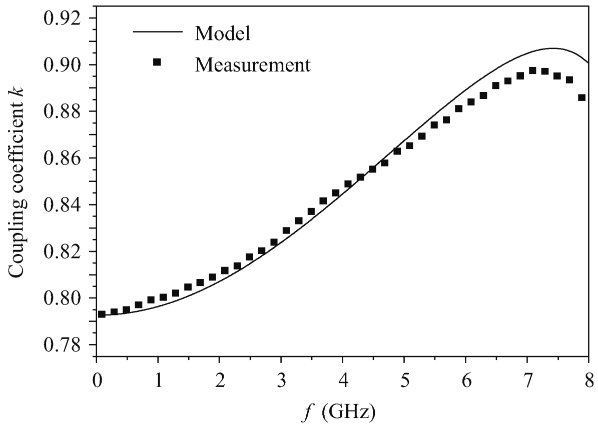

Fig. 11. Coupling coefficient comparison.

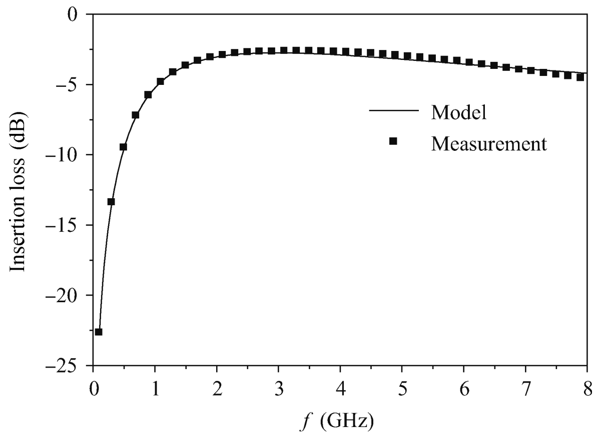

Fig. 12. Insertion loss comparison.

and simplifies the parameter extraction. By contrast, the parameter extraction of conventional models is much more difficult and sometimes needs the help of fitting and optimization.

6. Conclusion

A new compact T-model for spiral transformers has been presented. This 12-element-model can accurately capture the spiral transformer's electrical performances over a broad frequency range. Meanwhile, a simple parameter extraction procedure for the new model has also been introduced. In this procedure, a new method has been developed to extract the parameters of the ladder circuit without any optimization, and its application can be extended to the modeling of other passive components, such as on-chip transmission lines, inductors, and baluns.

References

[1] Sangsoo K, Jeong-Geun K, Taeksang S, et al. K- and Q-bands CMOS frequency sources with X-band quadrature VCO. IEEE Trans Microw Theory Tech, 2005, 53(9): 2789

[2] Simburger W, Wohlmuth H D, Weger P, et al. A monolithic transformer coupled 5-W silicon power amplifier with 59% PAE at 0.9 GHz. IEEE J Solid-State Circuits, 1999, 34(12): 1881

[3] Cassan D J, Long J R. A 1-V transformer-feedback low-noise amplifier for 5-GHz wireless LAN in 0.18 μm CMOS. IEEE J Solid-State Circuits, 2003, 38(3): 427

[4] Long J R. Monolithic transformers for silicon RFIC design. IEEE J Solid-State Circuits, 2000, 35(9): 1368

[5] Ng K T, Rejaei B, Burghartz J N. Substrate effects in monolithic RF transformers on silicon. IEEE Trans Microw Theory Tech, 2002, 50(1): 377

[6] El-Gharniti O, Kerherve E, Begueret J B. Modeling and characterization of on-chip transformers for silicon RFIC. IEEE Trans Microw Theory Tech, 2007, 55(4): 607

[7] Lin L, Yin W Y, Mao J F, et al. Performance characterization of circular silicon transformers. IEEE Trans Magnetics, 2008, 44(12): 4684

[8] Wang C, Liao H L, Xiong Y Z, et al. A physics-based equivalent-circuit model for on-chip symmetric transformers with accurate substrate modeling. IEEE Trans Microw Theory Tech, 2009, 57(4): 980

[9] Huailin L, Chuan W. A new approach to parameter extraction for on-chip symmetric transformers. IEEE International Symposium on Radio-Frequency Integration Technology, 2009: 257

[10] Mayevskiy Y, Watson A, Francis P, et al. A new compact model for monolithic transformers in silicon-based RFICs. IEEE Microw Wireless Compon Lett, 2005, 15(6): 419

[11] El-Gharniti O, Kerherve E, Begueret J B, et al. Modeling of integrated monolithic transformers for silicon RF IC. Proceedings of the 11th IEEE International Conference on Electronics, Circuits and Systems, 2004: 137

[12] H M Hsu, Tseng C W, Chan K Y. Characterization of on-chip transformer using microwave technique. IEEE Trans Electron Devices, 2008, 55(3): 833

[13] Huang F, Lu J, Jiang N, et al. Frequency-independent asymmetric double-π equivalent circuit for on-chip spiral inductors: physics-based modeling and parameter extraction. IEEE J Solid-State Circuits, 2006, 41(10): 2272

[14] Kim S, Neikirk D P. Compact equivalent circuit model for the skin effect. IEEE MTT-S International Microwave Symposium Digest, 1996, 3: 1815

[15] Lin Y S, Chen C Z, Liang H B, et al. High-performance on-chip transformers with partial polysilicon patterned ground shields (PGS). IEEE Trans Electron Devices, 2007, 54(1): 157